EEHG Performance and Scaling Laws

G. Penn

Center for Beam Physics, Lawrence Berkeley National Laboratory,
Berkeley, CA 94720, USA

October 2013

Published as NGLS Technical Note 35

This work was supported by the Director, Office of Science, Office of Basic Energy Sciences, of the U.S. Department of Energy under Contract No. DE-AC02-05CH11231.

EEHG Performance and Scaling Laws

G. Penn
Lawrence Berkeley National Laboratory

revised October 9, 2013

1 Introduction

This note will calculate the idealized performance of echo-enabled harmonic generation performance (EEHG) [1], explore the parameter settings, and look at constraints determined by incoherent synchrotron radiation (ISR) and intrabeam scattering (IBS). Another important effect, time-of-flight variations related to transverse emittance, is included here but without detailed explanation because it has been described previously [2]. The importance of ISR and IBS is that they lead to random energy shifts that lead to temporal shifts after the various beam manipulations required by the EEHG scheme. These effects give competing constraints on the beamline. For chicane magnets which are too compact for a given R_{56}, the magnetic fields will be sufficiently strong that ISR will blur out the complex phase space structure of the echo scheme to the point where the bunching is strongly suppressed. The effect of IBS is more omnipresent, and requires an overall compact beamline. It is particularly challenging for the second pulse in a two-color attosecond beamline, due to the long delay between the first energy modulation and the modulator for the second pulse.

2 A One-Dimensional Echo Calculation

Echo-enabled harmonic generation (EEHG) [1] operates through a form of wave-mixing, where two energy modulations are used instead of standard HGHG. In the most practical version of EEHG, the first modulation is followed by a chicane which severely overbunches the modulation, creating well-separated bands in longitudinal phase space. Each band has a very small energy spread and slow energy chirp, thus they are typically referred to as "energy bands". The second modulation is also followed by a chicane but in this case they are tuned so as to perform a standard phase rotation of each energy band. The low energy spread allows each band to achieve a high bunching factor even at very high harmonics. In addition, the multiple bands each generate bunching at different locations, not exactly evenly spaced but with good harmonic content. Each microbunch has the expected energy spread due to the modulation, but nearby microbunches have significant overlap in their range of energies. This allows the overall increase of energy spread to remain quite low,

because instead of being stacked in one large spike at the periodicity of the seed laser, they are staggered in longitudinal phase space and occupy overall a much smaller range of energy. This also greatly reduces the maximum local current present in the beam, compared to an HGHG scheme targeting a similar harmonic jump in one stage.

Here, we consider a fairly general case where the two seed lasers are both harmonics of some common wavelength, λ_0. We can then take the Fourier transform of the final particle distribution function in an idealized 1D case to obtain the resulting bunching factor. The final result will be the bunching factor averaged over the periodicity of the beam, λ_0. While this is typically the most important number for FELs where the beam radiates until it reaches saturation, it will generally not be useful for echo-based attosecond schemes [3, 4] where the beam radiates only over a short distance, or in the case where λ_0 is much larger than the slippage over the full length of the FEL. The following calculation is essentially the same as that by Stupakov [1], which was given for the specific case where the two seed lasers have identical wavelength; however, the variables and some of the "counting" indices have been chosen in a different way. In particular, the Bessel function indices are relabelled to make the groupings of harmonics with optimized bunching under the most typical configuration correspond to values of $m = 0,\ 1,\ 2,\ ...$ rather than to negative values. Also, the overall harmonic number, here denoted as h, has been restricted to be a non-negative integer, which changes most of the bunching parameters by a factor of 2.

Nonideal effects must be considered, especially any incoherent effects which may destroy the patterns generated in phase space. Such effects reduce the achievable bunching parameter, and it is not accurate to model energy spread due to ISR or IBS as any kind of effective increase in the original energy spread because the qualitative nature of the effect is too different. Although transverse-longitudinal coupling is not an incoherent effect, it has a similar effect on the bunching parameter [2]. This effect will be dealt with briefly below.

With these caveats, here is a derivation of the 1D formula for the generation of bunching through EEHG under ideal circumstances. The two seed lasers have wavelength λ_1 and λ_2, both harmonics of some wavelength λ_0. The final distribution is periodic in λ_0, and all Fourier components will be expressed in terms of harmonics h of λ_0, with h a non-negative integer. Thus we define these wavelengths in relation to each other as $\lambda_0 = n_1\lambda_1 = n_2\lambda_2 = h\lambda_X$, where n_1, n_2, and h are positive integers and λ_X is the wavelength of the harmonic we are interested in. We also define $k_0 = 2\pi/\lambda_0 = k_1/n_1 = k_2/n_2 = k_X/h$. In terms of its initial coordinates η_i and z_i, the first laser will modulate an electron to have relative energy deviation $\eta_1 = \eta_i + \eta_{m1}\sin[n_1(k_0 z_i + \psi_1)]$, where ψ_1 is defined in terms of the common periodic wavelength in order to avoid confusion when the wavelengths are different. The first chicane has a value of $R_{56} = R_1$, which moves the electron position to $z_1 = z_i + R_1\eta_1$. Combining yields

$$z_1 = z_i + R_1\left\{\eta_i + \eta_{m1}\sin\left[n_1(k_0 z_i + \psi_1)\right]\right\}. \tag{1}$$

Here, the sign convention is that "typical" chicanes, where high energy particles moves farther ahead, corresponds to positive R_{56}. But the derivation does not assume anything about R_{56}.

Similarly, the second laser changes the electron relative energy deviation to $\eta_2 = \eta_1 +$

$\eta_{m2}\sin[n_2(k_0 z_1+\psi_2)]$, and the second chicane with $R_{56}=R_2$ moves the electron position to

$$z_2 = z_1 + R_2\eta_2 = z_1 + R_2\left\{\eta_1 + \eta_{m2}\sin\left[n_2(k_0 z_1+\psi_2)\right]\right\}. \tag{2}$$

The Fourier components of the final particle distribution are

$$\hat{b}(h) = \langle \exp(-\mathrm{i}hk_0 z_2)\rangle = \int_{-\infty}^{\infty} \mathrm{d}\eta_i \frac{1}{2\pi}\int_0^{2\pi} \mathrm{d}\phi_i\, \exp(-\mathrm{i}hk_0 z_2), \tag{3}$$

where $\phi_i = k_0 z_i$, and each harmonic h corresponds to a wavelength λ_0/h. If we first replace z_2 with the variables at the end of stage 1, using Eq. (2), we find

$$\begin{aligned}
\exp(-\mathrm{i}hk_0 z_2) &= \exp\left\{-\mathrm{i}hk_0\left(z_1 + R_2\eta_1 + R_2\eta_{m2}\sin\left[n_2(k_0 z_1+\psi_2)\right]\right)\right\} \qquad (4)\\
&= \exp[-\mathrm{i}hk_0(z_1+R_2\eta_1)]\sum_{p=-\infty}^{\infty}(-1)^p J_p(hk_0R_2\eta_{m2})\exp\left[in_2p(k_0z_1+\psi_2)\right]\\
&= \sum_{p=-\infty}^{\infty}(-1)^p J_p(C_2\eta_{m2})\exp[-\mathrm{i}(h-n_2p)k_0z_1 - \mathrm{i}C_2\eta_1]\mathrm{e}^{in_2p\psi_2},
\end{aligned}$$

where the Bessel function sum was used to eliminate the sine term from the exponent, and $C_2 = hk_0R_2$. Now, if we expand z_1 and η_1 in terms of z_i and η_i, and combine terms, we obtain:

$$\begin{aligned}
\mathrm{e}^{-\mathrm{i}hk_0z_2} &= \sum_{p=-\infty}^{\infty}(-1)^p J_p(C_2\eta_{m2})\mathrm{e}^{-\mathrm{i}(h-n_2p)k_0z_i}\mathrm{e}^{\mathrm{i}n_2p\psi_2}\\
&\qquad\times\exp\{-\mathrm{i}C_1\eta_i - iC_1\eta_{m1}\sin\left[n_1(k_0z_i+\psi_1)\right]\}\\
&= \sum_{p=-\infty}^{\infty}(-1)^p J_p(C_2\eta_{m2})\sum_{m=-\infty}^{\infty}\mathrm{e}^{-\mathrm{i}(h-n_2p+n_1m)k_0z_i}\mathrm{e}^{\mathrm{i}(n_2p\psi_2-n_1m\psi_1)}\\
&\qquad\times J_m(C_1\eta_{m1})\mathrm{e}^{-\mathrm{i}C_1\eta_i}, \qquad (5)
\end{aligned}$$

where $C_1 = C_2 + k_0(h-n_2p)R_1 = k_0[hR_2 + (h-n_2p)R_1]$. Note that C_1 is a function not only of h, but of p as well. We can then integrate over $\phi_i = k_0 z_i$ to obtain the selection rule, $h = n_2p - n_1m$. The Bessel summation over m was chosen to have a different form from that over p, for the sole reason of choosing indices such that with positive h, and with positive values of R_{56}, the dominant terms will come from positive values of m and p. The final result is

$$\begin{aligned}
\hat{b}(h) &= \sum_{m\,\left|\,{}^{(h+n_1m)/n_2}_{=\text{ integer}}\right.} \mathrm{e}^{\mathrm{i}h\psi_2}\mathrm{e}^{\mathrm{i}n_1m(\psi_2-\psi_1)}(-1)^{(h+n_1m)/n_2}\\
&\qquad\times J_{(h+n_1m)/n_2}(C_2\eta_{m2})J_m(C_1\eta_{m1})\int \mathrm{d}\eta f_\eta(\eta)\mathrm{e}^{-\mathrm{i}C_1\eta}, \qquad (6)
\end{aligned}$$

where we can now set $C_1 = k_0(hR_2 - n_1mR_1)$. For an initial Gaussian energy distribution centered at $\bar{\eta}$,

$$\int \mathrm{d}\eta f_\eta(\eta)\mathrm{e}^{-\mathrm{i}C_1\eta} = \mathrm{e}^{-iC_1\bar{\eta}}\mathrm{e}^{-C_1^2\sigma_\eta^2/2}. \tag{7}$$

For simplicity, we will use the shorthand $p = (h + n_1 m)/n_2$, where p must be an integer for the term to count in the calculation in the overall Fourier component. The target wavelength then satisfies $hk_0 = pk_2 - mk_1$, and we will focus on cases where $p \gg m$. The bunching parameter for a given harmonic is simply the magnitude of $\hat{b}$.

3 Selecting Operating Parameters

Except for configurations with some extreme parameters or generating very low harmonics, each harmonic with significant bunching will be dominated by one term in the sum of Eq. (6). Thus, for a given harmonic, the various solutions can be characterized in terms of the value of m that contributes the most. Typically, m will be chosen to be small, so that $h \gg n_1 m$ or equivalently $\lambda_X \ll \lambda_1/m$. This is because the maximum value of the Bessel functions scales as one over the cube root of the index, so the bunching will scale as $m^{-1/3}[(h+n_1 m)/n_2]^{-1/3}$. For large h, we can thus either have a scaling as $h^{-1/3}$ if m is kept low, or if m is of order h then the overall scaling will go as $h^{-2/3}$ with a better coefficient but a much worse exponent. The only other alternative is to have $h+n_1 m$ itself be very small, but this essentially becomes a more complicated version of the standard HGHG scheme without any improvement in the scaling.

The two Bessel functions give a convenient separation between the parameters for the first stage and the second stage. The global maximum of the Bessel function of large index ν has a value roughly $0.67\,\nu^{-1/3}$. Because the second energy modulation, η_{m2}, only occurs in one place, it can be tuned to obtain exactly the optimum value of the large index Bessel function. The notation for the location of the global (and also first) maximum of the Bessel function is $j'_{\nu,1}$, which is given asymptotically for large positive ν by

$$j'_{\nu,1} \simeq \nu + 0.80861\,\nu^{1/3} + 0.07249\,\nu^{-1/3} - 0.05097\,\nu^{-1}. \tag{8}$$

The reason we take so many terms is because the performance is very sensitive to the parameters, especially η_{m2}. Getting close to the exact value greatly simplifies numerical analysis and allows one to skip fine tuning of the results (for $\nu > 100$, the last term can be dropped). Thus, we have one firm condition on an optimized beamline:

$$hk_0 R_2 \eta_{m2} = j'_{p,1}. \tag{9}$$

This gives a precise relationship between η_{m2} and R_2. For loose scaling laws, as opposed to setting precise values, we will approximate $j_{p,1} \simeq p$ and take $p = (h + n_1 m)/n_2 \approx h/n_2 = \lambda_2/\lambda_X$, even when this is not an integer. Then we find that

$$R_2 \simeq \frac{\lambda_2}{2\pi\eta_{m2}}\,, \qquad\qquad C_2 \simeq \frac{\lambda_2}{\lambda_X \eta_{m2}}\,. \tag{10}$$

The other terms all depend on the quantity $C_1 = k_0(hR_2 - n_1 m R_1)$ which combines terms from the two stages and can be tuned to be either positive or negative. The goal of the echo scheme is to make C_1 sufficiently small so that the Gaussian dependence on energy spread

does not kill the bunching, which requires $|hR_2 - n_1 m R_1| \ll hR_2$. On the other hand, if C_1 were exactly zero, then the remaining Bessel function term would yield zero bunching. Thus we have

$$R_1 \approx \frac{hR_2}{n_1 m} = \frac{R_2 \lambda_1}{m \lambda_X} \simeq \frac{\lambda_1 \lambda_2}{2\pi m \lambda_X \eta_{m2}}\,, \tag{11}$$

but this relation cannot be exact and still obtain bunching. For a given configuration, this results in a bunching spectrum which occupies a range of harmonics for each value m, but that drops down to zero bunching right in the center of that range.

The Bessel function J_m should be roughly optimized, yielding $|C_1|\eta_{m1} \simeq j'_{m,1}$. For the few, low values of m that will be considered, it is simplest just to use a table of values for $j'_{m,1}$, although the asymptotic expansion is not so bad either. However, for nonvanishing energy spread, some shift to lower argument will lead to a slightly better optimum. There will not be the sharp loss in bunching that the other Bessel function causes, but it is convenient to try to optimize the results as much as possible a priori. Maximizing the product

$$J_m(C_1\eta_{m1})\mathrm{e}^{-\sigma_\eta^2 C_1^2/2} \tag{12}$$

is equivalent to finding the solution to $J'_m(x) = (\sigma_\eta^2/\eta_{m1}^2)xJ_m(x)$, with $x = C_1\eta_{m1}$. Expecting the result to be close to $x = j'_{m,1}$, we can approximate the Bessel function as parabolic near its maximum. Using the standard differential equation which defines the Bessel functions, the second derivative at the maximum is equal to $J''_m(j'_{m,1}) = -[1-(m/j'_{m,1})^2]J_m(j'_{m,1})$. From this expression we obtain the first order correction to C_1,

$$C_1 \simeq \pm\frac{j'_{m,1}}{\eta_{m1}}\left[1 + \frac{\sigma_\eta^2}{\eta_{m1}^2}\frac{1}{1-(m/j'_{m,1})^2}\right]^{-1}. \tag{13}$$

Note that there are two solutions, reflecting the fact that the bunching spectrum has a double peak for each m value. For a given harmonic, the choice of positive C_1 yields a slightly smaller value of R_1, but the difference is almost insignificant. Using the above expressions for R_2 and C_1, which together also yields R_1, is sufficiently close to the exact optimum that no fine tuning is necessary except in the case of very large energy spread and thus extremely small bunching. Assuming the effect of energy spread is kept small, then the bunching is set by the maxima of the Bessel function terms, which are roughly given by $J_\nu(j'_{\nu,1}) \simeq 0.67\,\nu^{-1/3}$. Thus, the maximum achievable bunching for a given choice of m and $p \simeq h/n_2$ is roughly $0.45\,(n_2/hm)^{1/3} \simeq 0.45\,(\lambda_X/\lambda_2 m)^{1/3}$. The exponential term related to energy spread and non-ideal effects will further lower the actual bunching.

In practice, the undulators which generate the energy modulation also add dispersion, so the optimal values of R_{56} from the chicanes will be somewhat altered from these calculations. Although the effect should be relatively small, the high sensitivity of EEHG to the values of the dispersion makes these corrections important. In any event, tuning a real EEHG beamline will require scans in either chicane strength or laser strength to optimize the output radiation. Simulations will require either some additional tweaking from the expressions above or more accurate modeling of the beam dynamics in the undulator.

There are several important potential benefits from the fact that C_1 is typically much smaller than $2\pi R_2/\lambda_X$, which would be the comparable term for high gain harmonic generation (HGHG), and can be chosen to be either positive or negative. The reduced sensitivity of bunching parameter to initial energy spread means that high harmonics can be obtained from a relatively small ratio of energy modulation to bunching parameter. For even a cascade of HGHG steps to reach a large harmonic, it is generally necessary to resort to stages of "fresh bunch" delays [5] to move the radiation pulse away from regions of the electron bunch with energy spread that has been spoiled by previous interactions. In addition, longitudinal variations in the average electron energy will translate to phase shifts that are proportional to C_1, as seen in Eq. (7). These phase shifts will be much smaller than that of corresponding HGHG schemes and, if one chooses $C_1 < 0$, microbunches located in regions with higher energies will be shifted in phase *as if* they had been delayed in the chicanes rather than shifted forwards in time relative to electrons at the nominal energy. This is possible because of the complex two-wave mixing process which generates the targeted bunching. Following the EEHG stage, subsequent radiation or other beam manipulations will naturally tend to shift these microbunches back towards the nominal phase and nearly-perfect cancellation is possible, especially for energy variations with long length scales. For HGHG schemes, on the other hand, the only direct way to decrease these phase shifts is either to impose as large energy modulations as possible in the modulator, reducing the required strength of the dispersion in the chicane, or by building a complicated chicane with opposite dispersion from normal, and then adding ordinary dispersive elements in later stages to try to shift microbunches back to their nominal positions.

In terms of the remaining degrees of freedom, the strategy is to go to a stronger first energy modulation if one wishes to prevent the initial energy spread from lowering the bunching parameter, but once $\eta_{m1} > m\sigma_\eta$, there are diminishing returns. Or, one can reduce η_{m1} if desired and compensate by only changing R_1 to adjust the value of C_1. Similarly, one can trade off a smaller value of η_{m2} for a larger value of R_2, or the reverse.

4 Coupling to Transverse Dimensions

For the most part, the transverse properties of the electron beam has little effect on the performance of the EEHG beamline. We will see below how the transverse emittance and spot size affect scattering rates in a somewhat unintuitive way. There is also a requirement on the ratio of the spot size of the input lasers to that of the electron beam, related to the different field amplitudes encountered by electrons on axis and near the edge of the beam. Although this is a coherent effect, the coupling between energy and transverse coordinates eventually leads to a smearing of the bunching. Because the scaling with energy modulation enters in as the argument of Bessel functions, the required flatness of the field is related to the width of the maximum of the Bessel function, which scales as the cube root of the Bessel function index. As a rough estimate, for each modulation the bunching will be reduced by

a factor

$$1 - \frac{1}{1 + 3q^2/2 + q^4}\,, \tag{14}$$

where $q_1 = 1.26\, m^{-1/3}\sigma_{L1}/\sigma_{x1}$ and $q_2 = 1.26\, p^{-1/3}\sigma_{L2}/\sigma_{x2}$. The radius of the laser is defined in terms of power, and that of the electron beam in terms of density. Note that the GENESIS output for the radiation properties gives the rms radius of the electromagnetic field, which brings in an extra factor of $\sqrt{2}$. The reduction in bunching is about 0.96 for $q = 2$, 0.89 for $q = 1.5$, and 0.71 for $q = 1$. For the second energy modulation, where laser power requirements are often challenging, $q = 1.5$ seems to be a reasonable option. The size of the radiation mode is constrained to be greater than some multiple of the electron beam radius, and so here it will be treated as a fixed parameter. To preserve transverse uniformity, the undulator should be less than about 2 gain lengths, otherwise the radiation produced in the modulator by the beam will generate an additional transverse variation in field intensity.

For cases where the laser waist is sufficiently large that diffraction has little effect of the length of the modulator, we can adopt a simple estimate for the energy modulation created in a modulator by using a one-dimensional model with no FEL gain. For an undulator with length L_u, period λ_u, peak magnetic field on axis B_u, and dimensionless undulator parameter $a_u = eB_u\lambda_u/(2\pi\sqrt{2}\, m_e c)$, we can estimate the energy modulation as:

$$\eta_{m2} = \frac{1}{\gamma^2} L_u a_u \mathrm{JJ} \left(\frac{2r_e}{m_e c^3} \frac{P_L}{\sigma_L^2} \right)^{1/2}\,, \tag{15}$$

where P_L is the peak laser power, σ_L is the rms radius of the laser field (note that diffraction is ignored), and $\mathrm{JJ} \equiv J_0(\xi) - J_1(\xi)$ where $\xi = a_u^2/2(1 + a_u^2)$. This equation can also be used to obtain the required laser power for a given energy modulation.

There is another effect which becomes important as soon as the phase space structure contains longitudinal position scale lengths corresponding to the final output wavelength. This sensitivity happens by the end of the second undulator, and continues through the second chicane to the first undulators tuned to be resonant with the induced bunching, when the FEL gain process should compensate for any debunching. The problem in this stage is that the total path length, and thus time-of-flight, from the end of the second modulating undulator to the undulators tuned to produce x-rays will be different for electrons with different transverse coordinates [2]. Although this is a deterministic process, it still induces a blurring of the longitudinal phase space and thus can reduce the bunching. For a linear focusing system and ignoring coupling to dispersion, the transverse effects result in a spread of arrival times given by:

$$c^2 t_{\mathrm{RMS}}^2 = \left(1 + a_x^2\right) S_x^2 + \left(1 + a_y^2\right) S_y^2\,, \tag{16}$$

where

$$S_x \equiv \frac{\epsilon_{Nx}}{2\gamma} \int \mathrm{d}z\, \frac{1 + \alpha_x^2}{\beta_x} \tag{17}$$

and $0 \le a_x < 1$ represents the contribution from the different initial betatron phases of each electron and can also be expressed in terms of integrals over Twiss parameters and phase

advance. For a phase advance > 1 radian, a_x and a_y will typically be small and the arrival time is almost fixed by the transverse amplitudes alone. For very small phase advance a_x and a_y will be close to unity, and this is usually the worst case so a conservative estimate would take $a_x = a_y = 1$. The spread of arrival times is not Gaussian but instead starts at zero delay and increases with an exponential tail for large delays. The impact on the bunching is then a reduction by

$$\begin{aligned}\left|\frac{b}{b_{\rm ideal}}\right| &= \left\{\left[1+\left(1-a_x^2\right)\left(\frac{2\pi}{\lambda_X}\right)^2 S_x^2\right]^2 + 4a_x^2\left(\frac{2\pi}{\lambda_X}\right)^2 S_x^2\right\}^{-1/4} \\ &\times\left\{\left[1+\left(1-a_y^2\right)\left(\frac{2\pi}{\lambda_X}\right)^2 S_y^2\right]^2 + 4a_y^2\left(\frac{2\pi}{\lambda_X}\right)^2 S_y^2\right\}^{-1/4} . \end{aligned} \tag{18}$$

There is also a net phase shift. For the case $a_x \simeq a_y \simeq 0$ and similar horizontal and vertical terms, this yields a factor $1/[1+(2\pi S/\lambda_X)^2]$ or about $1-(2\pi S/\lambda_X)^2$ when the effect is small. For the case $a_x \simeq a_y \simeq 1$ we instead have a factor $[1+4(2\pi S/\lambda_X)^2]^{-1/2}$ or about $1-2(2\pi S/\lambda_X)^2$ when the effect is small. The limit where $a = 1$ is the worst case whenever $2\pi S/\lambda_X < 1$.

5 Random Energy Kicks

The importance of energy kicks such as from ISR and IBS depends on the location where the kicks occur. The effect of energy scattering on the entire phase space distribution has been considered in detail in [6]. It is simpler to focus narrowly on bunching at the target wavelength, and here we begin by considering an arbitrary position in the second chicane, which will be denoted as z_*. The transfer map from the beginning of the second chicane up to that point yields an R_{56} which will be written as $R(z_*)$. We consider a solitary stochastic kick for every electron, denoted as $\Delta\eta$. Then we have $z_* = z_1 + R(z_*)\eta_2$ and $\eta_* = \eta_2 + \Delta\eta$. The final parameters are now $z_f = z_* + [R_2 - R(z_*)]\eta_*$ and $\eta_f = \eta_*$. The exponential from Eq. (5) then becomes

$$\begin{aligned}\exp(-{\rm i}hk_0 z_f) &= \exp\left(-{\rm i}hk_0\left\{z_1 + R_2\eta_2 + [R_2 - R(z_*)]\Delta\eta\right\}\right) \\ &= \exp(-{\rm i}hk_0 z_2)\exp\left\{-{\rm i}hk_0[R_2 - R(z_*)]\Delta\eta\right\} . \end{aligned} \tag{19}$$

The only change from the previous calculation is the term $\exp\{-{\rm i}hk_0[R_2 - R(z_*)]\Delta\eta\}$; because $\Delta\eta$ is a stochastic parameter the expectation value will involve a decrease in magnitude of the bunching. It is reasonable as a first approximation to assume that all electrons scatter at the same rate, and in fact scattering is much more sensitive to the local current and transverse properties than to the individual electron energies. There could be a dependence on phase (the high-precision value of z_f) when microbunching is strong, which occurs both at the end of the second chicane and at various points in the first chicane as the beam overbunches, but here we take the rough approximation that all electrons in one region of

the electron beam will experience the same scattering rate, set to the average value. For a Gaussian distribution of $\Delta\eta$ with a possible offset, the bunching parameter will be multiplied by

$$\begin{aligned}\langle \exp\{-\mathrm{i}hk_0[R_2 - R(z_*)]\Delta\eta\}\rangle &= \exp\{-\mathrm{i}hk_0[R_2 - R(z_*)]\,\langle\Delta\eta\rangle\} \\ &\quad\times \exp\left\{-\frac{1}{2}h^2k_0^2[R_2 - R(z_*)]^2\eta_{\mathrm{RMS}}^2\right\}. \end{aligned} \tag{20}$$

If we apply the kick at different locations in the beamline, we get a similar result but with different expressions for the coefficient multiplying $\Delta\eta$. At the beginning of the beamline, the factor is simply $\exp(-\mathrm{i}C_1\Delta\eta)$, which matches the term $\exp(-\mathrm{i}C_1\eta_i)$ in Eq. (5). The calculation is slightly more complicated in the first chicane, because different p values (and therefore m values) in the sum will contribute differently, however we can usually focus on a single value of m. There is also an effect that the statistical noise of the scattering will increase Fourier components which would otherwise be very small, especially when the number of macroparticles is small. This effect tends to defeat the benefit of applying "quiet loading" to the initial macroparticle distribution in simulations.

Taking a single value of m, and assuming that the selection rule $h = n_2p - n_1m$ still holds, we find that the degradation in bunching is given by

$$\left\langle e^{-\mathrm{i}F(z)\Delta\eta}\right\rangle \simeq e^{-\mathrm{i}F(z)\langle\Delta\eta\rangle}e^{-\frac{1}{2}F^2(z)\eta_{\mathrm{RMS}}^2}, \tag{21}$$

where

$$F(z) = \begin{cases} C_1 & \text{before first chicane,} \\ C_1 + (C_2 - C_1)\frac{R(z)}{R_1} & \text{in first chicane,} \\ C_2 & \text{between chicanes,} \\ C_2\left(1 - \frac{R(z)}{R_2}\right) & \text{in second chicane,} \\ 0 & \text{after second chicane.} \end{cases} \tag{22}$$

Compared to C_2, C_1 is very small and can be ignored, because the energy kicks should not be anywhere near the original energy spread. The value of $C_2 = hk_0R_2 = 2\pi R_2/\lambda_X \simeq \lambda_2/(\lambda_X\eta_{m2})$.

For statistically independent kicks, the effects of those kicks at different locations add in quadrature, once variations in the weighting function are taken into account. We will replace discrete steps with an integral over distance along the beamline by setting

$$\langle\Delta\eta\rangle = \frac{\mathrm{d}\bar{\eta}}{\mathrm{d}z}\,\mathrm{d}z\,, \qquad \eta_{\mathrm{RMS}}^2 = \frac{\mathrm{d}\sigma_\eta^2}{\mathrm{d}z}\,\mathrm{d}z\,. \tag{23}$$

The bunching will then be given by

$$\begin{aligned}\frac{b}{b_{\mathrm{ideal}}} &= \exp\left[-i\int \mathrm{d}z\,F(z)\left(\frac{\mathrm{d}\bar{\eta}}{\mathrm{d}z}\right)_{\mathrm{ISR}}(z)\right] \\ &\quad\times\exp\left\{-\frac{1}{2}\int \mathrm{d}z\,F^2(z)\left[\left(\frac{\mathrm{d}\sigma_\eta^2}{\mathrm{d}z}\right)_{\mathrm{ISR}}(z) + \left(\frac{\mathrm{d}\sigma_\eta^2}{\mathrm{d}z}\right)_{\mathrm{IBS}}(z)\right]\right\}. \end{aligned} \tag{24}$$

We have used the fact that there is no average energy loss due to IBS. Other sources of scattering could be added to this calculation as well. For a non-Gaussian distribution of energy kicks, the averaging will lead to a slightly different formula for the degradation in bunching.

For the purpose of making analytic estimates, we will define the integrated quantities for typical energy loss and scatter across the entire chicane or other beamline element

$$\bar{\eta} \equiv \int \frac{\mathrm{d}\bar{\eta}}{\mathrm{d}z}\,\mathrm{d}z\,, \qquad\qquad \sigma_\eta^2 \equiv \int \frac{\mathrm{d}\sigma_\eta^2}{\mathrm{d}z}\,\mathrm{d}z\,. \tag{25}$$

For chicanes which are symmetric to avoid generating dispersion, we have the symmetry condition $R(z) + R(L-z) = R(L)$, where L is the length of the chicane. In this case, the phase term from ISR must be given by $C_2\bar{\eta}_{\rm ISR}/2$ (or more precisely replacing C_2 with C_2+C_1 for the first chicane). For the reduction in bunching, we can characterize the effect of the variation in $F(z)$ by writing

$$\int \mathrm{d}z\, F^2(z)\frac{\mathrm{d}\sigma_\eta^2}{\mathrm{d}z}(z) \equiv f C_2^2\sigma_\eta^2\,, \tag{26}$$

where f is a dimensionless scaling factor relating how this number compares to the equivalent scattering rate if $F(z)$ was pegged to its maximum value of C_2 throughout. The numerical value of f is not as straightforward as the previous calculation for average energy loss, but if both the chicane geometry and the scattering rate are symmetric across the chicane then we must have $1/4 \le f \le 1/2$. It is a fair approximation to take $f \simeq 3/8$ for any application. Note that the total amount of scattering must be calculated differently for ISR and IBS processes. For ISR, there is no scattering outside of the magnetic fields. For a chicane where dipoles have hard edges, the total scattering σ_η^2 should be the scattering rate for the peak magnetic field multiplied by $4L_M$, where L_M is the length of each dipole; for a planar undulator, the total scattering should be the peak scattering rate multiplied by $(4/3\pi)$ times the length of the undulator, where the numerical factor is because of the sinusoidally varying magnetic field. For IBS, in cases where the scattering rate is nearly constant over a beamline element, the total scattering is simply the scattering rate times the total length, including any drifts or matching sections. In between chicanes, such as where the second modulating undulator is located, F is a constant at C_2 so we simply have $f = 1$.

For a more explicit example of the value of f for chicanes, we take the chicane design assumed by GENESIS which has 4 identical dipoles with hard edges and 5 identical drifts (both between dipoles and at the start and end of the chicane). $R(z)$ grows with a cubic dependence in the dipoles and linearly in the drifts. If we only consider the contribution of path-length differences to $R(z)$ (ignoring terms proportional to $1/\gamma^2$), and treat the IBS scattering rate as a constant, we obtain the following expressions from Eq. (26):

$$f_{\rm IBS} \;=\; \frac{\frac{158}{7} + 99\frac{L_D}{L_M} + 144\frac{L_D^2}{L_M^2} + 69\frac{L_D^3}{L_M^3}}{64\left(1+\frac{5L_D}{4L_M}\right)\left(1+\frac{3L_D}{2L_M}\right)^2}\,,$$

$$f_{\rm ISR} = \frac{\frac{158}{7} + 69\frac{L_D}{L_M} + 54\frac{L_D^2}{L_M^2}}{64\left(1+\frac{3L_D}{2L_M}\right)^2}. \tag{27}$$

For both IBS and ISR, when $L_D \ll L_M$, this reduces to $79/224 \simeq 0.35$. In the limit where $L_D \gg L_M$, $f_{\rm IBS} = 23/60 \simeq 0.38$ and $f_{\rm ISR} = 3/8$. The entire range over all values of L_D/L_M is actually quite small, unless there is some drastic change in beam spot size or if the outer dipoles are significantly different than the inner dipoles.

6 Scaling Rules for Scattering

In either chicane, the effect of energy shifts on the bunching parameter is

$$\hat{b}_h \simeq \hat{b}_{h0} \exp\left(-\frac{\rm i}{2}C_2\bar{\eta}_{\rm ISR}\right) \exp\left[-\frac{1}{2}C_2^2\left(f_{\rm ISR}\sigma_{\eta\,\rm ISR}^2 + f_{\rm IBS}\sigma_{\eta\,\rm IBS}^2\right)\right]. \tag{28}$$

The average ISR energy loss across all four magnets of the chicane is

$$\bar{\eta}_{\rm ISR} = -\frac{2}{3}r_e\gamma(4L_M)\left(\frac{eB}{m_e v\gamma}\right)^2, \tag{29}$$

while fluctuations in ISR for the four magnets combined are given by

$$\sigma_{\eta\,\rm ISR}^2 = \frac{55r_e^2}{24\sqrt{3}\,\alpha}\gamma^5(4L_M)\left(\frac{eB}{m_e v\gamma}\right)^3. \tag{30}$$

Here, r_e is the classical electron radius, and α is the fine structure constant. These expressions are slightly different from that in, for example, the Handbook of Accelerator Physics and Engineering [7], because there everything is assumed to be averaged over synchrotron motion in a ring, and so half of the change in energy spread goes into the bunch width as the beam continues to match the shape of its RF bucket. For a typical chicane,

$$R_{56} = r\left(\frac{eB}{m_e v\gamma}\right)^2 L_M^3\frac{4}{3}\left(1+\frac{3L_D}{2L_M}\right), \tag{31}$$

where L_M is the length of each dipole, L_D is the length of the drift between dipoles, and r is a factor that allows for variation from the standard scaling as will be discussed below.

We could start with a scaling for ISR that is explicit in terms of the dependence on the magnetic field, something like $\sigma_{\eta\,\rm ISR}^2 = (4L_M/L_{\rm ISR}) \times [B/(1\text{ T})]^3$, but from Eq. (31) we can already see that we will be interested in the value of the quantity $1/\rho = eB/m_e v\gamma$, where ρ is the bending radius for the magnetic field. Thus we will use a more implicit expression,

$$\sigma_{\eta\,\rm ISR}^2 = \frac{4L_M d_{\rm ISR}^2}{\rho^3}, \tag{32}$$

where

$$d_{\rm ISR} \equiv r_e \left(\frac{55\gamma^5}{24\sqrt{3}\,\alpha} \right)^{1/2} . \tag{33}$$

In all of our scalings, we will consider changes in the chicanes where the ratio L_D/L_M is kept constant, so the last term in Eq. (31) will be treated as fixed. Whenever we choose to take derivatives over L_M, this ratio will still be considered as a constant. Taking this fixed ratio into account, we find that $R_{56} \propto L_M^3/\rho^2$, and so for a given R_{56}, we see that $\sigma^2_{\eta\,\rm ISR} \propto L_M^{-7/2}$. We define L_s as being the magnet length such that ISR in one chicane causes the bunching factor to degrade by a factor $e^{-1/2}$, so that

$$\left| \frac{b}{b_{\rm ideal}} \right|_{\rm ISR} = \exp\left[-\frac{1}{2} \left(\frac{L_s}{L_M} \right)^{7/2} \right] . \tag{34}$$

There will be separate values L_{s1} and L_{s2} for each chicane. By expressing the dipole field in terms of the resulting R_{56}, we find that

$$L_{sj} = \left[4 f_{\rm ISR} C_2^2 d_{\rm ISR}^2 \left(\frac{3}{4 r_j (1 + 3L_{Dj}/2L_{Mj})} R_j \right)^{3/2} \right]^{2/7} , \tag{35}$$

where $j = 1, 2$ depending on the chicane being considered. If either chicane has dipoles significantly shorter than the corresponding L_s, bunching will be practically eliminated, considering the large exponent in Eq. (34). Because R_1 is much larger than R_2, we expect L_{s1} to be more of a constraint with $L_{s2}/L_{s1} \simeq (R_2/R_1)^{3/7} \simeq (\lambda_1/m\lambda_X)^{3/7} \ll 1$, using earlier approximations for R_1 and R_2 Therefore it is worth substituting in for the first chicane explicitly to obtain

$$\begin{aligned} L_{s1} &= \left[4 f_{\rm ISR} d_{\rm ISR}^2 \left(\frac{2\pi R_2}{\lambda_X} \right)^2 \left(\frac{3 R_1}{4 r_1 (1 + 3L_{D1}/2L_{M1})} \right)^{3/2} \right]^{2/7} \\ &\simeq \left(\frac{\lambda_2}{\lambda_X \eta_{m2}} \right) \left(\frac{\lambda_1}{2\pi m r_1} \right)^{3/7} \left[4 f_{\rm ISR} d_{\rm ISR}^2 \left(\frac{3}{4 r_1 (1 + 3L_{D1}/2L_{M1})} \right)^{3/2} \right]^{2/7} . \end{aligned} \tag{36}$$

L_{s1} has some dependence on λ_1/mr_1, but more significant is the fact that it is proportional to $\lambda_2/\lambda_X\eta_{m2}$. This suggests that the difficulty of an EEHG beamline scales with the ratio between the wavelengths of the second external laser and the desired output laser, but this can be ameliorated by increasing the second energy modulation, at least until the total energy spread becomes too large to be practical. Below, we will drop the factors r_1 and r_2, but it is worth considering that if $r_1 = 2$, in other words for an unconventional chicane design with twice as much dispersion for the same dipoles, then the dipole lengths could be reduced by about 25%, and $r_1 = 5$ would give roughly a 50% reduction. Chicanes containing quadrupoles for changing the value or even sign of R_{56} are not uncommon, but they do add complexity and may require fixed field values. We shall see that the effect of IBS is not

directly reduced by using larger m or r_1, but anything which allows the first chicane to be shorter will help.

The effect of scattering in the first modulating undulator should be negligible, it simply increases the initial energy spread. However, in the second modulating undulator, the phase space is already very sensitive to energy diffusion. The peak magnetic field B_u satisfies $\rho_u = m_e v\gamma/eB_u = \lambda_u v\gamma/(2\pi\sqrt{2}\,ca_u)$, and the effect of averaging a scattering rate that goes like $|\rho_u^{-3}|$ over a sinusoidally varying field gives a factor of $4/3\pi$. Thus, for the second undulator, $\sigma^2_{\eta\,\mathrm{ISR}} = 4L_u d^2_{\mathrm{ISR}}/(3\pi\rho_u^3)$. The corresponding reduction in bunching due to ISR is $\exp[-(1/2)C_2^2\sigma^2_{\eta\,\mathrm{ISR}}]$. The argument of the exponent scales as $L_u(\lambda_2/\lambda_X\eta_{m2})^2\rho_u^{-3}$, where L_u is the length of the undulator.

The effect of IBS is more difficult to ameliorate because it always grows with distance travelled by the beam. This pushes the design to be as compact as possible, which conflicts with the requirements imposed by ISR. For a cylindrically symmetric beam, the rate of energy spread growth due to IBS is roughly [8]:

$$\left(\frac{\mathrm{d}\sigma_\eta^2}{\mathrm{d}z}\right)_{\mathrm{IBS}} \simeq \frac{\pi^{1/2}}{2}\ln\Lambda\,\frac{I}{I_A}\frac{r_e}{\gamma^2\sigma_x\epsilon_N}\,, \tag{37}$$

if we take an average over transverse co-ordinates. Note the dependence on rms spot size, which will vary with beam optics. Here, $I_A = ec/r_e \simeq 17045$ A is the Alfvén current. The argument Λ of the Coulomb logarithm may commonly be defined as the density times the volume of a Debye sphere, with radius λ_D. This is probably an over-estimate of scattering as we are using rms scattering angles including rare, large collisions, and this is also the expression for a large volume whereas for typical FEL parameters the plasma Debye length will be larger than the beam radius. Given that the electron beam in the rest frame is typically long and narrow, we consider instead the actual number of electrons which are within a longitudinal distance of $\pm\lambda_D$ in the rest frame. In addition, we can optionally cut off large individual scattering events that kick electrons outside of the FEL bandwidth. This changes the argument of the logarithm from $2/\chi_{\min}$ to $\chi_{\max}/\chi_{\min}$, where $\chi_{\max} \simeq \rho_{\mathrm{FEL}}\beta/\gamma\sigma_x$. The factor multiplying the FEL parameter (here standing in for the cutoff in relative energy kick) is equivalent to $c/\sigma_{v\perp}$ in the rest frame. Thus we should consider the following possible expressions:

$$\Lambda = \begin{cases} \frac{4\pi}{3}n_{e0}\lambda_D^3 = \frac{\sqrt{2}}{6}\frac{\epsilon_N^3}{r_e\sigma_x^2}\left(\frac{I}{I_A}\right)^{-1/2}, & \text{homogeneous} \\ \frac{2\lambda_D}{\gamma}\frac{I}{ec}\,, & \text{narrow beam} \\ \frac{2\lambda_D}{\gamma}\frac{I}{ec}\frac{\rho_{\mathrm{FEL}}\beta}{2\gamma\sigma_x}\,, & \text{with cutoff.} \end{cases} \tag{38}$$

Here, n_{e0} and λ_D are the electron density and Debye length in the rest frame, and other quantities are calculated in the lab frame. The cutoff can actually have a significant effect, because in the rest frame the transverse velocities are almost always below the speed of light but the ratio is usually not as low as typical FEL parameters ($\sim 10^{-3}$).

Similar to Eq. (32), we define the scattering across some beamline element as

$$\sigma^2_{\eta\,\mathrm{IBS}} = \frac{L}{L_{\mathrm{IBS}}}\left(\frac{\beta_{\mathrm{nom}}}{\beta}\right)^{1/2}, \tag{39}$$

where we note the fact that $\sigma_x = (\epsilon_N \beta/\gamma)^{1/2}$ and treat any changes in the beta function as a scaling from some nominal value because the dependence is fairly weak. Thus,

$$L_{\rm IBS} = \frac{2}{\pi^{1/2}\,\ln\Lambda}\frac{\epsilon_N^{3/2}\gamma^{3/2}\beta_{\rm nom}^{1/2}}{r_e I/I_A}\,. \tag{40}$$

To keep dimensions of length, large $L_{\rm IBS}$ corresponds to small scattering rates, while large $d_{\rm ISR}$ corresponds to large scattering rates. The scaling with beam energy is partially an artifact because of the normalization to relative energy spread.

The total effect within a chicane can be expressed as

$$\left|\frac{b}{b_{\rm ideal}}\right|_{\rm IBS} = \exp\left(-L_M/2L_b\right)\,, \tag{41}$$

with

$$L_b = \frac{L_{\rm IBS}}{4f_{\rm IBS}C_2^2}\left(1+\frac{5L_D}{4L_M}\right)^{-1}\left(\frac{\beta}{\beta_{\rm nom}}\right)^{1/2} \simeq \frac{L_{\rm IBS}}{4f_{\rm IBS}}\left(1+\frac{5L_D}{4L_M}\right)^{-1}\left(\frac{\lambda_2}{\lambda_X\eta_{m2}}\right)^{-2}\left(\frac{\beta}{\beta_{\rm nom}}\right)^{1/2}. \tag{42}$$

Here we assume the chicane is configured so that its total length is $4L_M + 5L_D$. The first and last drift, as well as the drift in the center of the chicane, are essentially wasted space but in the limit where $L_D \ll L_M$ the net impact should be small. Again note that unlike for ISR, large values of L_b are better. The dependence on the beta function is weak, especially compared to the dependence on η_{m2} and λ_2. There is no explicit benefit to going to smaller λ_1 or larger m, although anything which allows the total length of the chicanes to be reduced will help. Higher peak current and smaller emittance make scattering worse by increasing the electron density.

The phase space in the second undulator is also sensitive to IBS, just as it is to ISR. The degradation in bunching has the same form, $\exp[-(1/2)C_2^2\sigma_{\eta\,\rm IBS}^2]$, but now $\sigma_{\eta\,\rm IBS}^2 = (\beta_{\rm nom}/\beta)^{1/2}L_{\rm between}/2L_{\rm IBS}$. The total distance between chicanes, $L_{\rm between}$, will include both the second modulator and any drift or matching regions. For the purpose of optimizations we will assume a constant ratio $L_{\rm between}/L_u$, similar to the ratio between drifts and dipoles in the chicanes. The factor in the exponent thus scales as $L_u(\lambda_2/\lambda_X\eta_{m2})^2(\beta_{\rm nom}/\beta)^{1/2}$.

7 Optimizations

For a given target wavelength, the main parameters to consider are the seed laser wavelengths, the height of the energy modulations, and the preferred value of the parameter m. Alternatively, the height of the second energy modulation can be treated as dependent on the strength of the second chicane.

There are two main operating regimes to be considered. To generate an attosecond spike, we cannot take advantage of the FEL gain because slippage will increase the pulse duration. The main optimization in this case is to apply as much energy modulation as

possible, because we are not worried about the final energy spread. This gives maximum local bunching plus enhanced current where bunching is greatest. The second seed laser will have to be a few-cycle pulse with a controlled carrier-envelope relative phase, although perhaps something useful could be obtained by having the first seed laser be the short pulse instead. Another important optimization to maximize the number of photons is to try to compress the beam transversely to a smallest spot size (highest electron density). However, both IBS and coupling between time of flight and transverse coordinates are worse for compressed beams.

For a long seeded pulse, it will be desirable for the bunched beam (typically at a few % bunching) to undergo FEL gain until saturation is reached. The main optimization in this case is to keep the final energy spread at least a few times smaller than the Pierce parameter, and preferably many times smaller in order to produce significant radiation at harmonics. The first energy modulation must be at least a few times larger than the energy spread, while if the second energy modulation is too small, the first chicane will have to be very strong, with long magnets to minimize ISR.

For the chicanes, the dependence on the length of the dipole magnets is already eliminated in the definitions of L_s and L_b. The total chicane length is again assumed to be $4L_M(1 + 5L_D/4L_M)$ where the ratio L_D/L_M is considered fixed. Thus for each chicane, the combined loss of bunching will be:

$$\exp\left[-\frac{L_M}{2L_b} - \frac{1}{2}\left(\frac{L_s}{L_M}\right)^{7/2}\right] . \tag{43}$$

Because of the much higher sensitivity to L_M of the second term, the optimum value of L_M will occur when the term of the exponent from IBS is 7/2 times the value from ISR. This optimum value satisfies

$$L_M^{9/2} = \frac{7}{2} L_s^{7/2} L_b \, . \tag{44}$$

The corresponding decrease in bunching is

$$\left|\frac{b}{b_{\rm ideal}}\right|_{\rm chicane} = \exp\left(-\frac{9}{14}\frac{L_M}{L_b}\right) = \exp\left[-\frac{9}{4}\left(\frac{2L_s}{7L_b}\right)^{7/9}\right] . \tag{45}$$

Thus, to avoid significant degradation we want $L_s \ll L_b$, which makes sense because the constraint is for L_M to lie roughly between these values.

Specifically, for the first chicane which is the more challenging case, we see from previous approximations for C_2 and R_1 that the optimum value for the dipole length scales as

$$L_{M1} \propto \left(\frac{\lambda_2}{\lambda_X \eta_{m2}}\right)^{1/3} \left(\frac{\lambda_1}{m}\right)^{1/3} \left(\frac{\beta}{\beta_{\rm nom}}\right)^{1/9} , \tag{46}$$

while the term in the exponent for the reduction in bunching scales as

$$\left(\frac{\lambda_2}{\lambda_X \eta_{m2}}\right)^{7/3} \left(\frac{\lambda_1}{m}\right)^{1/3} \left(\frac{\beta}{\beta_{\rm nom}}\right)^{-7/18} . \tag{47}$$

The scaling in η_{m2} lies in between the individual scalings for ISR, $(L_M\eta_{m2})^{-7/2}$, and for IBS, $L_M\eta_{m2}^{-2}$.

It is possible to significantly reduce the impact of scattering and improve the performance of the beamline by increasing the second energy modulation. In a manner similar to Eq. (34), we can describe the dependence on energy modulation by writing

$$\left|\frac{b}{b_{\rm ideal}}\right|_{\rm chicane\ 1} = \exp\left[-\left(\frac{\eta_{\rm ch}}{\eta_{m2}}\right)^{7/3}\right], \tag{48}$$

where the quantity $\eta_{\rm ch}$ is the value of the second energy modulation which would give a reduction in bunching by a factor of $1/e$ in the first chicane, assuming that the magnet length in the first chicane is re-optimized for each value of energy modulation. We choose a factor of $1/e$ because the effects of ISR and IBS are combined in this calculation. Clearly, if the energy modulation is below this value, the bunching will be severely degraded, although the scaling is slightly less bad than that found previously for dipole length. Expanding out this result, we find that

$$\begin{aligned}\eta_{\rm ch} &= \eta_{m2}\left(\frac{9}{4}\right)^{3/7}\left(\frac{2L_{s1}}{7L_{b1}}\right)^{1/3} \qquad (49)\\ &\simeq 3\frac{\lambda_2}{\lambda_X}\left(\frac{\lambda_1}{2\pi m}\right)^{1/7}\left(\frac{\beta_{\rm nom}}{\beta}\right)^{1/6}\frac{(1+5L_{D1}/4L_{M1})^{1/3}}{(1+3L_{D1}/2L_{M1})^{1/7}}\left(\frac{f_{\rm IBS}}{7L_{\rm IBS}}\right)^{1/3}\left(\sqrt{2}\,f_{\rm ISR}d_{\rm ISR}^2\right)^{2/21}.\end{aligned}$$

The above scaling is rather painful for improving performance using λ_1, m, and β, although every little bit helps. In practice, it appears to almost always be best to use $m = 1$ because for energy modulations large enough to achieve good results, the increase in idealized bunching when $m = 1$ more than makes up for any improvement that comes directly from reducing the required values of R_{56}. There is also only a weak dependence on the value of the Coulomb logarithm once the optimization procedure is viewed as choosing the energy modulation, which provides some excuse for the very rough derivation of the IBS scattering rate. For a given beam ratio of λ_2/λ_X, the minimum energy modulation in the second undulator is almost already set. The dependence on beam energy is especially weak, in total scaling only as $\gamma^{-1/42}$! The sensitivity to energy modulation can be reduced more effectively by either lowering the beam current or increasing the transverse emittance (because larger relative velocities reduce the scattering rate); the modulation parameter $\eta_{\rm ch}$ scales as $I^{1/3}\epsilon_N^{-1/2}$. These changes also have only a modest penalty in terms of final saturation power.

As stated above, this condition on the energy modulation set by the first chicane will be more restrictive than that set by the second chicane. The constraints set by the second modulator, on the other hand, have a different scaling so it is useful to further explore this effect. By combining the effects of IBS and ISR in the region in between the two chicanes, the loss of bunching will be:

$$\exp\left\{-\frac{1}{2}C_2^2\left[\frac{L_{\rm between}}{L_{\rm IBS}}\left(\frac{\beta_{\rm nom}}{\beta}\right)^{1/2}+\frac{4L_u d_{\rm ISR}^2}{3\pi\rho_u^3}\right]\right\}. \tag{50}$$

For a fixed physical layout and without any optimizations both terms scale as η_{m2}^{-2}, so we can write this as

$$\left|\frac{b}{b_{\rm ideal}}\right|_{\rm undulator\ 2} = \exp\left[-\left(\frac{\eta_{\rm und0}}{\eta_{m2}}\right)^2\right], \tag{51}$$

where

$$\eta_{\rm und0}^2 \simeq \frac{L_u}{2}\left(\frac{\lambda_2}{\lambda_X}\right)^2\left[\frac{L_{\rm between}}{L_u}\frac{1}{L_{\rm IBS}}\left(\frac{\beta_{\rm nom}}{\beta}\right)^{1/2} + \frac{4d_{\rm ISR}^2}{3\pi\rho_u^3}\right]. \tag{52}$$

For the second undulator the main parameters are the undulator length, undulator period, undulator parameter, and the bending radius corresponding to the peak magnetic field. These are related by definition such that $\rho_u = \lambda_u v\gamma/(2\pi\sqrt{2}\,ca_u)$, and constrained by the resonance condition $\lambda_2/\lambda_u = (1+a_u^2)/2\gamma^2$, leaving two free parameters. It turns out that exploring a full two-dimensional optimization for a fixed energy modulation is not useful, because it is always optimal to have the shortest possible undulator. However, that is only because the laser power creating the modulation is being allowed to increase without constraint.

Thus, it is necessary to consider the relationship of laser power to the applied energy modulation. We can obtain at least a rough estimate for the energy modulation from a given laser power from Eq. (15), which is more accurate for shorter modulators. If we consider fixing the laser power, this still leaves two free parameters if the energy modulation is allowed to vary. This scaling eliminates the problem that $L_u \to 0$ appeared to be optimal, because the energy modulation will also shrink and the bunching will actually go to zero. However there is again a false optimum, this time for very long undulators, because the bunching parameter continuously improves but only because the energy modulation becomes arbitarily large. In practice, there are good reasons for wanting the energy modulation to stay low, in particular it should be lower than the FEL energy acceptance of the targeted output wavelength λ_X. Therefore, it makes more sense to restrict the parameter space by considering both a fixed laser power and a fixed energy modulation, leaving only one degree of freedom. Through Eq. (15), we can rewrite the reduction in bunching in terms of laser power, energy modulation, and undulator parameter to yield

$$\begin{aligned}\left|\frac{b}{b_{\rm ideal}}\right|_{\rm undulator\ 2} = \exp\Bigg\{ &-\frac{\gamma^2}{2}\eta_{m2}C_2^2\left(\frac{2r_e}{m_ec^3}\frac{P_L}{\sigma_L^2}\right)^{-1/2} \\ &\times\frac{1}{a_u{\rm JJ}}\left[\frac{L_{\rm between}}{L_u}\frac{1}{L_{\rm IBS}}\left(\frac{\beta_{\rm nom}}{\beta}\right)^{1/2} + \frac{4d_{\rm ISR}^2}{3\pi}\left(\frac{\pi\sqrt{2}\,c}{\lambda_2 v\gamma^3}\right)^3 a_u^3\left(1+a_u^2\right)^3\right]\Bigg\}.\end{aligned} \tag{53}$$

The exponent scales as $\eta_{m2}^{-1}P_L^{-1/2}$. The undulator length is prescribed by Eq. (15). Moreover, the optimization of undulator parameter a_u does not have any dependence on the energy modulation or laser power, just the ratio between IBS and ISR scattering rates and the wavelength of the second seed laser. Even the dependence on beta function is extremely weak. The optimization is especially straightforward if one ignores the variation of JJ; this

is a reasonable approximation when the undulator parameter is large, which is typical for modulators. The optimum undulator parameter is then the one for which the ISR term in the brackets is equal to the IBS term multiplied by $(1 + a_u^2)/2(1 + 4a_u^2)$, or about 1/8 for $a_u \gg 1$. The reduction in bunching for the optimized value of a_u is

$$\left|\frac{b}{b_{\rm ideal}}\right|_{\rm undulator\ 2} \simeq \exp\left[-\frac{\gamma^2}{2}\frac{1}{\eta_{m2}}\left(\frac{\lambda_2}{\lambda_X}\right)^2\left(\frac{2r_e}{m_e c^3}\frac{P_L}{\sigma_L^2}\right)^{-1/2} \times \frac{3}{2a_u \text{JJ}}\frac{1+3a_u^2}{1+4a_u^2}\frac{L_{\rm between}}{L_u}\frac{1}{L_{\rm IBS}}\left(\frac{\beta_{\rm nom}}{\beta}\right)^{1/2}\right]. \tag{54}$$

We can use this expression to scale the reduction in bunching as either $\exp(-P_{\rm und}^{1/2}/P_L^{1/2})$, where $P_{\rm und}$ is proportional to $1/\eta_{m2}^2$, or $\exp(-\eta_{\rm und}/\eta_{m2})$, where $\eta_{\rm und}$ is proportional to $P_L^{-1/2}$ which is in turn inversely proportional to the originally specified undulator length. Note that these optimizations only consider the effect of scatter in between the chicanes, and may be overridden by the effects of scattering in the chicanes themselves.

One important case where we cannot approximate the distance between the chicanes as being comparable to the length of the second undulator is for the two-color attosecond beamline. After the first chicane, the second pulse does not even begin to be generated until the first pulse has already been radiated. Therefore, a much longer distance between chicanes should be considered. Another difference for attosecond beamlines is that the second undulator is restricted to be one or at most two undulator periods to generate a sufficiently narrow energy modulation. Thus, the above scalings for fixed laser power should be replaced by $L_u = N_u\lambda_u$, where N_u is fixed. This already leaves only one degree of freedom so the laser power must be allowed to vary for a given energy modulation, but the optimum a_u in this case is fairly similar and again independent of the actual value of the energy modulation; the ISR term in the exponent must be equal to the IBS term multiplied by $2a_u^2/(3+7a_u^2)$. For $a_u \gg 1$ the optimum a_u in terms of bunching parameter for a given energy modulation should be about 10% larger than the optimum calculated previously, and the undulator period about 17% smaller. If available laser power is a limiting factor, then a longer undulator period would be needed.

8 Application to Specific Parameters

We consider the application of this analysis to two types of beamlines based on the EEHG scheme. A summary of the electron beam and laser parameters are given in Tables 1 and 2. Note that the predicted bunching ignores degradation due to the transverse size of the laser. This can be made very minimal in the first undulator, but is more challenging in the second undulator, where the effect is estimated to be around 10%. The beta function everywhere is also pessimistically chosen as the value in the radiating undulators, it is possible to increase this value upstream of this point to reduce IBS, but this is not worth it if the required optics signicantly increases the beamline length. The best design would be to not have

Table 1: Sample parameters for an echo beamline producing long x-ray pulses based on Ref. [9].

General Parameters		
Bunch charge	300 pC	
Energy	1800 MeV	
Peak current	500 A	
Emittance	0.6 micron	
Nominal beta	10 m	
Target wavelength	1.2 nm	
EEHG or Modified Parameters		
	Original	**Modified**
Energy spread	0.05 MeV	0.15 MeV
Seed wavelength 1	200 nm	200 nm
Modulation 1	0.167 MeV	0.4 MeV
Laser power 1	1.9 MW	2.6 MW
Seed wavelength 2	200 nm	200 nm
Modulation 2	0.333 MeV	0.8 MeV
Laser power 2	140 MW	315 MW
m parameter	2	1
Chicane 1 R_{56}	14.3 mm	12.0 mm
Chicane 1 magnets	1.5 m	0.75 m
Chicane 1 drifts	0.5 m	0.25 m
Chicane 2 R_{56}	179 μm	74.0 μm
Chicane 2 magnets	0.5 m	0.25 m
Chicane 2 drifts	0.5 m	0.25 m
Undulator 2 period	0.20 m	0.20 m
Undulator 2 length	1 m	1.6 m
Distance between chicanes	1.75 m	2.35 m
Predicted bunching without IBS	0.035	0.051
Predicted bunching with IBS	3.5×10^{-5}	0.022

Table 2: Sample parameters for an echo beamline for attosecond pulses, and potentially producing two pulses with independent photon energies. Original design did not take IBS into account.

General Parameters			
Bunch charge		300 pC	
Energy		2400 MeV	
Energy spread		0.15 MeV	
Peak current		500 A	
Emittance		0.6 micron	
Nominal beta		6 m	
Target wavelength		1.2 nm	
Attosecond EEHG Parameters			
	Original	**800 nm seed**	**400 nm seed**
Seed wavelength 1	267 nm	267 nm	267 nm
Modulation 1	0.6 MeV	0.6 MeV	0.6 MeV
Laser power 1	54 MW	8.5 MW	17 MW
Seed wavelength 2	800 nm	800 nm	400 nm
Modulation 2	1.8 MeV	3.6 MeV	2.4 MeV
Laser power 2	23.2 GW	23.1 GW	13.0 GW
m parameter	2	1	1
Chicane 1 R_{56}	18.8 mm	18.7 mm	14.0 mm
Chicane 1 magnets	2.5 m	1.50 m	1.50 m
Chicane 1 drifts	0.5 m	0.25 m	0.25 m
Chicane 2 R_{56}	173 μm	86.2 μm	65.0 μm
Chicane 2 magnets	0.5 m	0.25 m	0.25 m
Chicane 2 drifts	0.5 m	0.25 m	0.25 m
Undulator 2 period	0.50 m	1.0 m	1.0 m
Undulator 2 length	0.25 m	1.0 m	1.0 m
Distance between chicanes	1.0 m	1.75 m	1.75 m
Predicted bunching without IBS	0.021	0.034	0.047
Predicted bunching with IBS	6.5×10^{-5}	0.012	0.026

any quadrupoles at all between the first chicane and the first x-ray producing undulator. The quoted peak power requirements for the lasers are approximate, and especially for the few-cycle laser used for attosecond pulses are going to be underestimates by a significant amount, as diffraction and the fall-off in the beam envelope even over one wavelength of slippage become important.

The first beamline is a generic seeded FEL based on the example of Ref. [9], where ISR was modeled but IBS was neglected. Both seed lasers have a wavelength of 200 nm, and harmonic number 165 is targeted for a wavelength of roughly 1.2 nm. The original design is modified based on the optimizations already given, and in particular we examine how much the energy modulation needs to be increased just to accomodate IBS. For the modified example, the energy spread has been allowed to become much larger because for the increased energy modulation there is no need to require such a low energy spread. The impact of ISR from the original study was controlled by lengthing the chicane dipoles, but as shown this only pushes IBS into the forefront. The purpose is to see how high a photon energy one can produce with the shortest seed laser wavelength wavelength ($\approx$ 200 nm) compatible with conventional laser technology.

More effort could be put into eliminating needless space between chicanes, and to reconfigure the optics to eliminate the quadrupole after the second undulator. This would increase bunching to 0.025. It is generally advantageous to have short drifts and long dipoles with low magnetic fields. The optimum dipole length would be 0.8 m, but for a dipole length so close to this optimum the difference in final bunching is negligible. The undulator period optimization is similarly soft, especially if the undulator period is made longer, as long as one pays attention to laser power requirements. The optimum undulator period is 0.15 m, but 0.20 m has been selected to leave room to push to even higher harmonics; the performance is the same but the required laser power is 315 MW instead of 269 MW.

Phase space images of the beam for the two long-pulse EEHG examples are shown in Figure 1, both after the first chicane and after the second chicane. The effect of scattering has been removed in generating these images. In simulations, the power of the second laser and dipole strengths are reasonably close to the predicted values, though not exact. The laser size was slightly smaller than it should be because the Rayleigh length was rounded off to 4 m, and some dispersion is already created in the undulators. For the original design, the bands in energy are separated by about 25 keV after the first chicane. However, because $m = 2$ was chosen in this design, this energy separation actually transforms into 2.4 nm distance upon phase rotation. The bunching at 1.2 nm is significant because the individual bunches are sufficiently narrow. An electron which receives a 6 keV energy kick will thus be almost exactly out of phase from where it would otherwise be inside the x-ray producing undulator tuned to 1.2 nm. The more meaningful energy gap is thus $12.5\,\mathrm{keV} = (1/m) \times 25\,\mathrm{keV}$. The rms energy kick required to reduce the overall bunching by $1/e$ is then $12.5\,\mathrm{keV}\,/(\pi\sqrt{2}) \simeq 2.8\,\mathrm{keV}$. This is close to the energy kick due to IBS after 1 m.

For the modified design, the energy bands are separated by 30 keV, which is only different from the original case because of the slightly reduced dispersion in the first chicane. There are more energy bands due to the increased energy modulation, and because we have

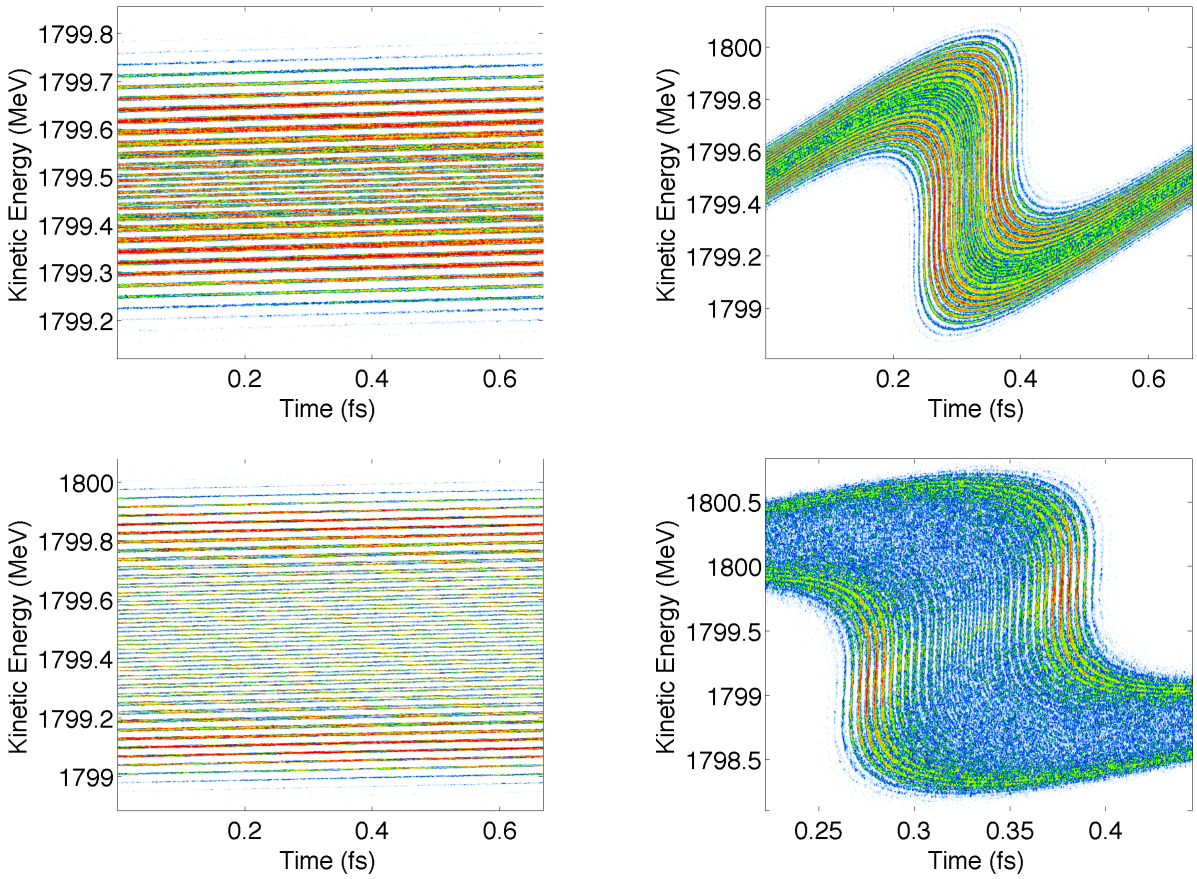

Figure 1: Longitudinal phase space density plots for the original (top) and modified (bottom) long-pulse EEHG configurations, with scattering neglected. After the first chicane (left), the bands in energy space are separated by ≈ 25 keV and 30 keV respectively. After the second chicane (right), the bunches are separated by 2.4 nm and 1.2 nm. The final phase space plot in the modified configuration shows less than one wavelength to reveal the finer detail.

selected parameters for $m = 1$, the individual bunches after the second chicane are separated by 1.2 nm. Thus, it takes an energy kick of 15 keV to shift a single electron out of phase, compared to 6 keV for the original case, and this design is significantly more robust to scattering. The rms energy kick required to reduce the overall bunching by $1/e$ is $30\,\mathrm{keV}/(\pi\sqrt{2}) \simeq 6.8\,\mathrm{keV}$. It takes more than 5 m of beamline for IBS to produce an rms energy kick of this magnitude.

The second example is an attosecond pulse using a few-cycle laser for the second energy modulation similar to the example of Ref. [4]. The beam parameters are based on the current design for the Next Generation Light Source [10], and the initial design did not take IBS into account. This scheme allows two pulses at two different photon energies to be produced by repeating the second energy modulation and subsequent radiating undulator, with slightly different parameters. Here, a longer seed wavelength was used because the best few-cycle

lasers currently available operate in the IR. Ameliorating this is the fact that the attosecond pulse is produced without relying on FEL gain, so there is almost no restriction on the amplitude of the energy modulations except for the laser technology itself. There is an additional issue from the long distance between the first chicane and the final chicane used as part of generating the second laser pulse. This is not a fundamental problem as in theory the complete attosecond beamline could be repeated twice, but it would be simpler to only perform the initial beam "striping" once. Three examples are shown: an initial design effort which did not take IBS into account, and two redesigns to accomodate the effects of IBS. In the original design, the wavelength of the first seed laser is 267 nm and that of the second seed laser is 800 nm. Harmonic number 660 is targeted for a wavelength of roughly 1.2 nm. One design option simply increases the energy modulation as before, while the other uses less laser power but reduces the wavelength of the second seed laser to 400 nm. Because of the mode selection rule, the output wavelength is targeted to be 800/661 nm $\simeq$ 1.2 nm. Both cases not only reduce the sensitivity to scatter but allow for shorter magnets in the first chicane.

The final bunching produced in the attosecond beamline is not exactly the proper target parameter, because we are interested in the local bunching parameter over a single current spike produced after the second chicane, rather than the average over a longer region of the electron beam. The local bunching parameter isolated in that single spike can be almost an order of magnitude larger for large energy modulations, and the enhanced local current also helps to produce more radiation power, but the average bunching is still useful as a rough figure of merit. Sub-femtosecond x-ray pulses which can be produced for these parameters seem limited to approximately 10^7 photons, although the pulse durations can be as short as 100 attoseconds. Using a few-cycle seed laser at 400 nm seems to be a large improvement, but the ability to produce such pulses is uncertain, and the efficiency in producing such pulses compared to those at 800 nm is significantly lower. Reducing the wavelength of the first seed laser to 200 nm has a negligible impact in the performance. To produce two pulses, there must be a significant distance between the first chicane and the last chicane, within which the first x-ray pulse will be produced. A key figure of merit is then the decay in bunching due to IBS for the second bunch. The length of beamline for IBS to degrade the final bunching by a factor of $e^{-1/2}$ is 0.62 m, 2.5 m, and 4.4 m for the three cases given in Table 2. Multiplying these numbers by $2\ln 2 \simeq 1.39$ gives the equivalent "half-life" of the bunching. Clearly, the option with a 400-nm seed laser would be best for a two-pulse beamline. The energy modulation may even have to be made larger in order to accomodate not only the second chicane and last two modulators, but also to be able to refocus the beam down to a small beta function in the final radiating undulator in order to maximize the number of photons.

We list some key parameters for the EEHG schemes and for the effects of ISR and IBS, including those properties in the frame moving with the electron beam which are important for IBS. Here, we focus on the long-pulse EEHG examples. For an idealized beam, the radius of the bunch is 41 micron, the rms bunch duration is 240 fs, and the relative energy spread is 2.8×10^{-5} for the original example and 8.3×10^{-5} for the modified example. The

transverse momentum spread is 0.015 $m_e c$. In the rest frame of the beam, the transverse momentum spread is still 0.015 $m_e c$ and the longitudinal momentum spread is 2.8×10^{-5} $m_e c$ and 8.3×10^{-5} $m_e c$ for the two examples. Also in the rest frame, the bunch length is 0.25 m, the peak density is 2.8×10^{17}, and the corresponding Debye length (taking the transverse temperature) is 150 micron. Note that this is significantly larger than the transverse radius. The value of the Coulomb logarithm for the three expressions given in Eq. (38) are 15.1, 13.7, and 10.3. These expressions yield order unity variations whose accuracy cannot be taken too seriously, and we have not considered the fact that the distribution is not strictly Gaussian. The smallest of these values has been used in the calculations, yielding an IBS scattering rate of 2.8 keV in 1 m, adding in quadrature.

The parameters of the modified example are sufficiently close to the optimum values for the increased energy modulation that the final bunching parameter is not affected by the difference. The total scattering from IBS in the first chicane, second undulator, and second chicane are 5.8 keV, 4.3 keV, and 4.2 keV, respectively. The corresponding factors for the reduction in bunching in these beamline elements are 0.76, 0.65, and 0.86. The equivalent numbers for ISR are 3.6 keV, 0.6 keV, and 0.4 keV, and 0.90, 0.99, and 1.00.

Although IBS appears to be the dominant effect degrading the performance of all of the beamlines considered, this is in reality due to the nature of the competition between IBS and ISR. Because the rate of energy spread due to ISR is so sensitive to magnetic field strength, while IBS is relatively insensitive to everything but total beamline length, the optimum configuration always has contributions from ISR which are a factor of 3.5 to 8 times lower than that of IBS. However, the physics of ISR is just as important as that of IBS in determining the optimal parameters and thus setting the corresponding performance.

9 Summary

The theory of EEHG has been described in a convenient formalism with optimized parameters defined by a small set of input parameters. In addition, a large assortment of non-ideal effects which can degrade performance have been evaluated and used to obtain further optimizations in beamline design. It is particularly important to consider energy scattering due to both ISR and IBS, because these effects act in competing ways to constrain the design parameters. Either source of scattering individually could be worked around, but in combination the only way to achieve high harmonic jumps is to increase the amount of energy modulation imposed on the electron bunch. The amount and statistical properties of energy scattering produced by IBS in a short beamline is not very well understood, and may be especially complicated within chicanes and undulators. Although the final requirements imposed by IBS on beamline design have been shown to have a modest dependence on the precise scattering rate, it is an interesting problem in basic beam physics. Specific designs for the basic EEHG scheme and attosecond pulses have been considered. The attosecond scheme in particular is very demanding and its performance is limited by the lack of FEL gain; however, the x-ray pulses produced may still be useful for specialized applications.

References

[1] G. Stupakov, "Using the Beam-Echo Effect for Generation of Short-Wavelength Radiation", Phys. Rev. Lett. **102** (2009) 074801.

[2] C.S. Sun, H. Nishimura, G. Penn, M. Reinsch, D. Robin, F. Sannibale, C. Steier, W. Wan, "Study of highly isochronous beamlines for FEL seeding", in Proceedings of FEL2011 (Shanghai, China, 2011), WEPB02 pp. 391–393.

[3] D. Xiang, Z. Huang, and G. Stupakov, "Generation of intense attosecond x-ray pulses using ultraviolet laser induced microbunching in electron beams", Phys. Rev. ST Accel. Beams **12** (2009) 060701.

[4] A. Zholents and G. Penn, "Obtaining two attosecond pulses for X-ray stimulated Raman spectroscopy", Nucl. Instrum. Methods A **612** (2010) 254–259.

[5] L.H. Yu and I. Ben-Zvi, "High-gain harmonic generation of soft X-rays with the 'fresh' bunch technique", Nucl. Instrum. Methods A **393** (1997).

[6] G. Stupakov, "Effect of Coulomb collisions on echo-enabled harmonic generation (EEHG)", in Proceedings of FEL2011 (Shanghai, China, 2011), MOPB20 pp. 49–52.

[7] *Handbook of Accelerator Physics and Engineering*, A.W. Chao and M. Tigner, eds., World Scientific, Singapore, 2006.

[8] Z. Huang, "Intrabeam Scattering in an X-ray FEL Driver", SLAC report LCLS-TN-02-8, November 2002.

[9] G. Penn and M. Reinsch, "Designs and numerical calculations for echo-enabled harmonic generation at very high harmonics", Journal of Modern Optics **58** (2011) 1404–1418.

[10] J.N. Corlett et al., "Next Generation Light Source R&D and Design Studies at LBNL", in Proceedings of IPAC2012 (New Orleans, USA, 2012), TUPPP070 pp. 1762–1764.